PROCEEDINGS OF SCIENCE

Large-amplitude intraday variability in QSO 1156+295 observed during a VLBI experiment

Tuomas Savolainen[*a] **and Yuri Y. Kovalev**[ab]
[a]*Max-Planck-Institut für Radioastronomie*
Auf dem Hügel 69, 53121 Bonn, Germany
[b]*Astro Space Center of Lebedev Physical Institute*
Profsoyuznaya 84/32, 117997 Moscow, Russia
E-mail: tsavolainen@mpifr-bonn.mpg.de, ykovalev@mpifr-bonn.mpg.de

We present here the discovery of rapid, large amplitude intraday variability in the compact flat-spectrum radio quasar 1156+295. The detection of 40% flux density variations at 15 GHz on a timescale of only 2.7 hours was serendipitously made when the source was observed with the Very Long Baseline Array as a part of the MOJAVE survey programme on February 5, 2007. Intraday variability on timescales of a few hours or less is rare, and there exist very few sources that show large-amplitude variations on a timescale as short as what is now observed for 1156+295. The shape of the visibility function of the source changes very little during the observation, although the correlated flux density changes by 40%. This suggests that the variability occurs in a single dominant compact component. The observed variability characteristics are consistent with interstellar scintillation in nearby, highly turbulent medium. The rms amplitude of modulation at 15 GHz is unusually large and it implies a rather high scattering measure along the line-of-sight towards 1156+295.

Workshop on Blazar Variability across the Electromagnetic Spectrum
April 22-25 2008
Palaiseau, France

*Speaker.

PoS(BLAZARS2008)062

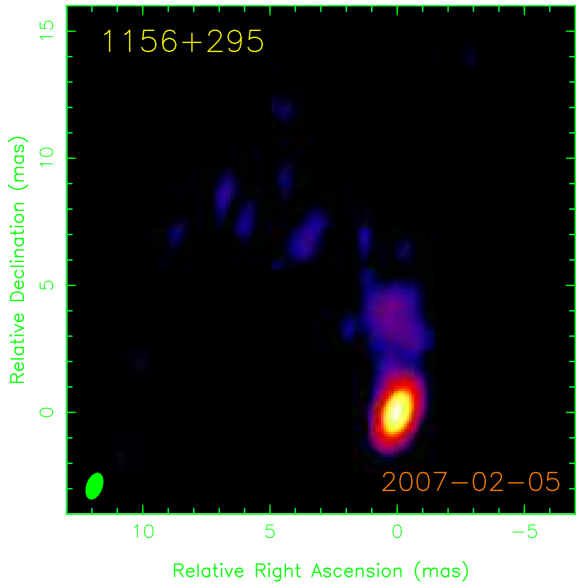

Figure 1: Naturally weighted 15 GHz false colour image of 1156+295 observed with the VLBA on February 5, 2007. The map peak brightness is 1.46 Jy beam^{-1} and the low flux density cut-off is at 0.7 mJy beam^{-1}.

1. Introduction

Flux density variations on timescales of $\lesssim 2$ days – so-called intraday variability (IDV) – are seen at centimetre wavelengths in a significant fraction of compact, flat-spectrum AGN [19, 13]. There is now good evidence that, at least in the case of the most extreme sources showing large-amplitude variations on intra-hour timescales, the IDV is due to interstellar scintillation (ISS) in the turbulent, ionised interstellar medium[1] (see e.g. [3] and references therein). This evidence is mainly based on the detection of time delays in the variability pattern arrival times between widely separated telescopes and on the observations of an annual modulation of the variability timescale. By detailed analysis of the scintillation it is possible to probe both the ISM and the structure of compact radio sources at microarcsecond resolution, which is far higher than what can be achieved by the present day VLBI [14]. The short variability timescale of the most extreme sources facilitates such studies by allowing well-sampled observations of the flux density fluctuations to be made within a single observing run. Unfortunately, however, while IDV in flat-spectrum radio sources is common, variability on timescales of a few hours or less and with an rms amplitude of modulation larger than 10% is extremely rare and only a handful of such sources are known. We report here the serendipitous discovery of one new source, QSO 1156+295, showing IDV on a timescale of less than 3 h and with 13% rms amplitude of modulation. This discovery is unusual in two ways. Firstly, it was made during a VLBI experiment, and secondly, the modulation index of 13% is atypically high at 15 GHz.

2. Observations and analysis

1156+295 (4C +29.45) is a quasar at $z = 0.729$ that is strongly variable throughout its spectrum

[1] We note that there are some sources likely exhibiting also intrinsic variability on a timescale of ~ 1 day [16].

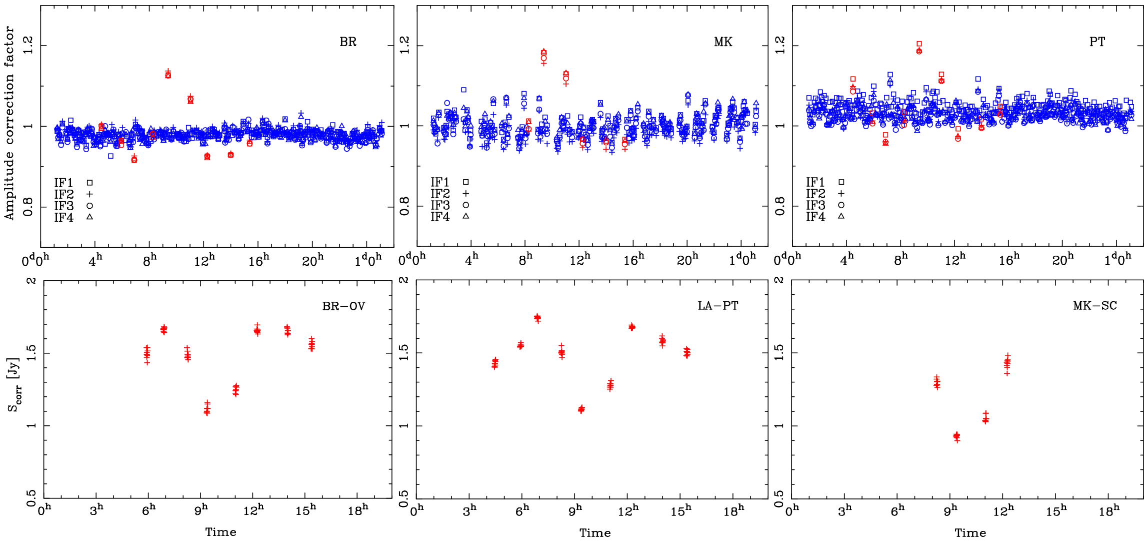

Figure 2: *Top:* Amplitude self-calibration solutions of three example antennas (BR, MK, and PT) for the VLBA observation on February 5, 2007. The figure shows one solution per scan and per IF. Scans at elevations below 15° are excluded. Solutions for 1156+295 are shown in red colour, while blue colour corresponds to the solutions of all the other sources. The obvious discrepancy between the solutions for 1156+295 and for the other sources is present at all ten antennas. *Bottom:* Examples of the correlated flux density curves of 1156+295 at three baselines after calibration of antenna gains by amplitude correction factors interpolated from the nearby scans of other sources. Interpolation was done from the scans that were within 1 h of the target scan, and that were observed at source elevation $> 15°$. Time is in UT.

from radio to gamma-rays [10, 20, 18]. It has a core-jet morphology in VLBI maps and it appeared strongly core-dominated in 2007 (Fig. 1). 1156+295 was observed with the NRAO's Very Long Baseline Array (VLBA) at 15 GHz as a part of the MOJAVE project [12] on February 5, 2007. In the same 24-hour session, 24 other sources beside 1156+295 were also observed. The individual scans of different sources were interleaved in order to maximise the (u,v) coverage for each source. 1156+295 was observed for 9 scans distributed between 4^h and 16^h UT and each lasting 4.7 min. The data were calibrated using the standard methods of VLBI data reduction (see description in [12]). After *a priori* amplitude calibration and fringe fitting, it was noticed that the correlated flux density of 1156+295 shows strong, correlated temporal variability from scan to scan at *every baseline*. There is a deep minimum, surrounded symmetrically by two maxima, in the correlated flux density curves between 7^h and 12^h UT. The peak-to-trough amplitude of this dip is 0.6 Jy, 40% of the average flux density, and the variability timescale is only 2.7 h. The dip can be seen at every baseline, which excludes the source structure as the cause of the variability. Also, neither the system temperature measurements used in the amplitude calibration nor the fringe-fit solutions of the experiment showed any anomalies that could explain the variability as an instrumental effect.

We tested the reality of the flux density variations by imaging and self-calibrating the (u,v) data of 1156+295 in a usual manner and comparing the resulting antenna gain correction factors with those derived from the self-calibration of the other 24 sources observed in the same experiment. The top panels in Fig. 2 show these gain amplitude correction factors for three example antennas. While the amplitude self-calibration with a 5-minute solution interval is able to remove

PoS(BLAZARS2008)062

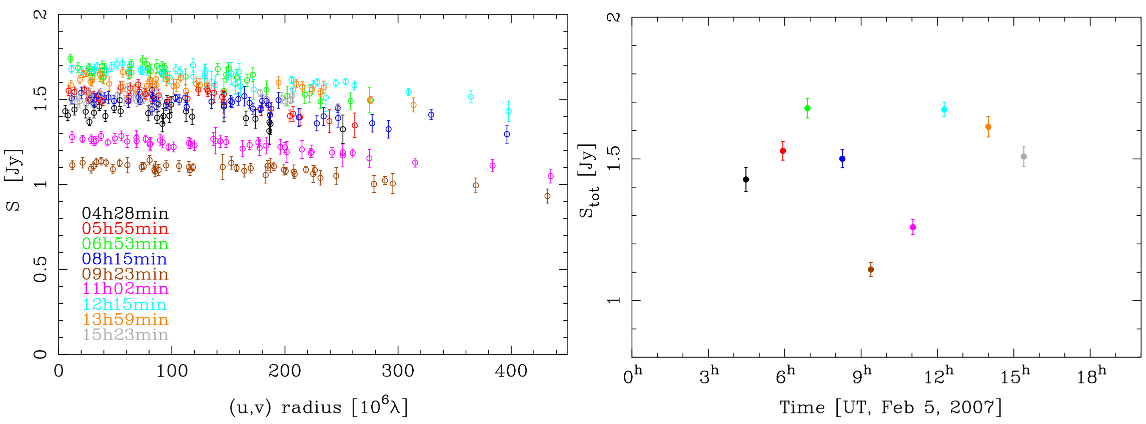

Figure 3: *Left:* Calibrated correlated Stokes I flux density of 1156+295 as a function of (u,v) radius for each individual scan of the VLBI experiment on February 5, 2007. The data has been averaged over the IFs and over the scan length in time. The different scans are shown in different colours with the scan start time in UT indicated in the legend. *Right:* Integrated flux density curve of 1156+295, obtained by averaging the visibility amplitudes at projected baselines shorter than 100 Mλ. The colour-coding of the scans corresponds to the one used in the left panel.

the variability in 1156+295, it results in gain amplitude correction factors that are – *for every antenna* – significantly offset from those determined from the 24 other sources. This can be explained if the observed variability is indeed genuine IDV, but does not significantly change the shape of the source's visibility function during the observation. This happens for example when the variability occurs in a single dominant, compact component. Calibration errors cannot account for the behaviour described above, because the antenna gain is source-independent. Thus, we conclude that the variations in the correlated flux density of 1156+295 are due to genuine IDV.

The residual errors in the antenna gains, which remain after the *a priori* amplitude calibration, need to be corrected before the observed variability in 1156+295 can be properly analysed. The large number of sources that were observed during the MOJAVE session allow us to estimate the gain amplitude correction factors for 1156+295 by interpolating the self-calibration solutions from the nearby scans of other sources. Examples of correlated flux density curves that were calibrated in this way are shown in the bottom panels of Fig. 2. As can be seen in the figure, the variations in the correlated flux density are very similar at long (MK-SC), intermediate (BR-OV), and short (LA-PT) baselines. The left panel of Fig. 3 shows the calibrated correlated flux density of 1156+295 as a function of (u,v) spacing for each individual scan. The figure suggests the shape of the visibility function does not change appreciably during the observation, although the flux density changes by 40%. To quantify this, we have plotted in Fig. 4 the difference between the normalised visibility function of each scan and the average visibility function of the whole observation of 1156+295. There are small changes, on the level of $<$ 8%, in the shape of the visibility function during the observation. However, as can be seen in the right panel of Fig. 4, these changes are purely due to the baselines to one antenna (St. Croix), and they can be caused by calibration inaccuracies of this antenna. We therefore cannot claim time variability in the shape of the visibility function. In any case, such variability is on the level below 8% during the course of observation.

The right panel of Fig. 3 shows the integrated VLBA flux density curve for 1156+295, which

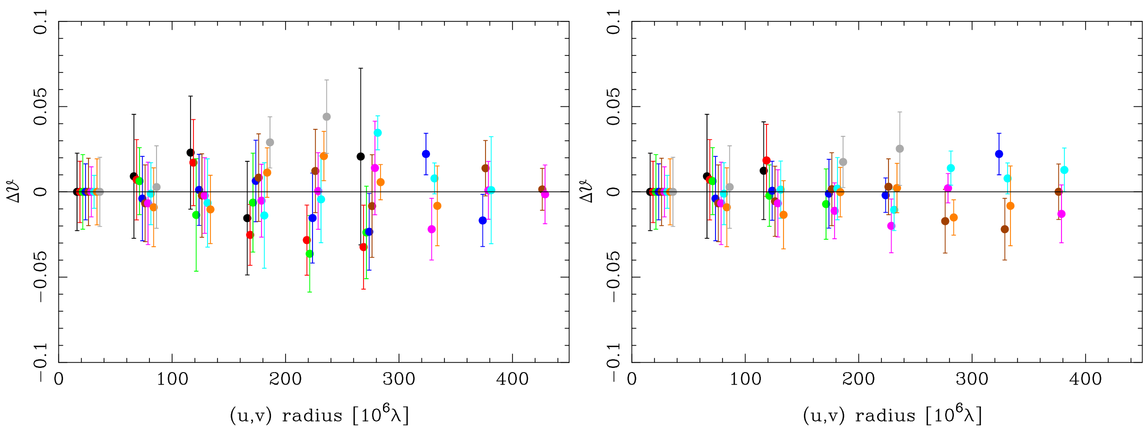

Figure 4: *Left:* Difference between the visibility function of each individual scan of 1156+295 and the average, binned visibility function of the whole observation. The visibility function is obtained by normalising the binned correlated flux density of each scan to the value in its first (u,v) radius bin. The bin size is 50 Mλ. The scans are shown with the same colour-coding as in Fig. 3. As can be seen, there is very little change in the normalised visibility function despite the strong variability of the correlated flux density. During the observation, the normalised visibility function changes at (u,v) radius of $200-300$ Mλ, but only less than 8%. *Right:* Same as in the left panel, but without baselines to St. Croix. Now the small changes in the shape of the visibility function during the observation have completely vanished.

we constructed by averaging the visibility amplitudes at projected baselines between $6-100$ Mλ. Since the visibility function is essentially flat in this range (see the left panel of Fig. 3), the averaging gives a good estimate of the integrated emission coming from angular scales $\lesssim 30$ mas. Averaging also reduces the errors that are due to inaccurate amplitude calibration, since these are antenna-specific. From the integrated VLBA flux density curve, we calculate the variability timescale as the average of the peak-to-trough and trough-to-peak times of the big dip, which gives $t_{\rm var} = 2.7 \pm 0.5$ h. The modulation index m, defined as the standard deviation of the flux density curve divided by the mean flux density, is 13 ± 3%. This value of m is much higher than what is typically observed for IDV sources at frequencies above 5 GHz [7, 11].

3. Discussion

Through light-travel time arguments, the variability timescale of 2.7 hours translates into a brightness temperature of $\gtrsim 2 \times 10^{19}$ K for 1156+295 if the observed flux density variations are source-intrinsic. This is far in excess of the inverse Compton (IC) catastrophe limit of 10^{12} K [8]. Therefore, a very high Doppler factor would be needed in order to explain the observations in the standard framework of incoherent synchrotron radiation from a jet of relativistic electrons. A Doppler factor of $\gtrsim 270$ would be needed in order to avoid the IC catastrophe in the case of a power-law electron energy distribution, and even in the case of the quasi-monoenergetic electron population [9], a Doppler factor of $\gtrsim 200$ would be needed. Such fast jets are unlikely to exist on both theoretical [1] and observational [4] grounds. Thus, we consider it probable that the fast variability observed in 1156+295 is due to source-extrinsic effects.

A sufficiently compact radio source will scintillate due to the wave propagation effects in the ionised interstellar medium of our Galaxy (for a review, see e.g. [15, 6]). The scattering strength is determined by the strength of the electron density fluctuations along the line of sight. Below a certain critical frequency $\nu_{\rm s}$, both narrow-band diffractive and broad-band refractive scattering phenomena can be observed and the scattering is referred to as "strong". Above the critical frequency, in the so-called "weak" scattering regime, the refractive and diffractive scattering length scales become equal and flux density variations arise due to slight focusing and defocusing over the Fresnel scale.

The variability timescale and modulation index can be used to constrain the properties of the scattering medium. IDV has been previously observed in 1156+295 at 5 GHz in 2002, albeit with less extreme characteristics: $m = 5.8\%$ and $t_{\rm var} \sim 20$ h have been reported [13]. For a point source, $m \propto \nu^{17/30}$ and $t_{\rm var} \propto \nu^{-11/5}$ in the case of strong refractive ISS, while in the weak regime $m \propto \nu^{-17/12}$ and $t_{\rm var} \propto \nu^{-1/2}$ [15]. Therefore, the difference between timescales observed at 5 GHz and 15 GHz suggests that $\nu_{\rm s}$ is above 5 GHz. This implies a rather large scattering measure towards 1156+295, which is somewhat unexpected considering the high galactic latitude ($b = 78.4^\circ$) of the source [5]. However, if the scintillation occurs in the very local ISM, there is not necessary a strong correlation between the scattering measure and the galactic latitude [2]. There are also 5 years between these observations, and the source could have been in a more compact stage at our epoch than in 2002. Simultaneous multifrequency measurements are needed to settle this.

Setting a lower limit to the intrinsic source size, $\theta_{\rm s}^{FWHM}$, by the IC catastrophe argument, it is possible to constrain the maximum distance to the scattering screen. If the maximum Doppler factor δ is assumed to be < 50 [4], the lower limit to $\theta_{\rm s}^{FWHM}$ is about 17 μas. Together with the short variability timescale of 2.7 h and the modulation index of 13%, this implies a maximum screen distance of about 300 pc for typical screen velocities [6, 17]. If equipartition conditions in the source are assumed, we can estimate that $\theta_{\rm s}^{FWHM} \sim 270 \cdot \delta^{-7/17}$ μas. Again assuming $\delta < 50$, this would place the screen at the distance of $\lesssim 100$ pc. The above calculations constrain also the scattering measure [6], which indeed turns out to be rather large: $SM \gtrsim 0.5\,{\rm m}^{-20/3}$ pc for a screen distance of $\lesssim 300$ pc, and $SM \gtrsim 4\,{\rm m}^{-20/3}$ pc for a screen distance of $\lesssim 100$ pc (an uncertainty of 3% in m has been assumed when calculating these limits; a more detailed analysis is presented in [17]).

The rapid, large amplitude IDV in 1156+295 is in principle consistent with interstellar scintillation due to a nearby, localised region of highly turbulent ionised gas. The above-derived lower limits for *SM* in the direction of 1156+295 are, however, 5-40 times larger than what is predicted by Cordes & Lazio [5] model of the distribution of free electrons in the Milky Way. Therefore, further observations should be carried out to search for other signs of increased turbulence in the direction of 1156+295. Finally, we note that the case of 1156+295 is also an important reminder that large amplitude IDV within the timescale of a VLBI experiment violates the basic assumption made in Earth rotation synthesis, and can significantly degrade VLBI imaging results.

Acknowledgments

We thank Lars Fuhrmann, David Jauncey, Thomas Krichbaum, Matthew Lister and Sarma Kuchibhotla for useful discussions. Both authors are research fellows of the Alexander von Humboldt Foundation. TS was also partially supported by the Max-Planck-Gesellschaft and by the Academy of Finland grant 120516. The National Radio Astronomy Observatory is a facility of the National Science Foundation operated under cooperative agreement by Associated Universities, Inc.

References

[1] M. C. Begelman, et al. 1994, *Energetic and radiative constraints on highly relativistic jets*, *ApJ* **429**, 57

[2] N. D. Ramesh Bhat, et al. 1998, *Pulsar Scintillation and the Local Bubble*, *ApJ* **500**, 262

[3] H. E. Bignall, et al. 2007, *Observations of intrahour variable quasars: scattering in our Galactic neighbourhood*, *A&AT* **26**, 567

[4] M. H. Cohen, et al. 2007, *Relativistic Beaming and the Intrinsic Properties of Extragalactic Radio Jets*, *ApJ* **658**, 232

[5] J. M. Cordes & T. J. W. Lazio 2002, *NE2001.I. A New Model for the Galactic Distribution of Free Electrons and its Fluctuations*, [astro-ph/0207156]

[6] J. Goodman 1997, *Radio scintillation of gamma-ray-burst afterglows*, *New Astronomy* **2**, 449

[7] L. L. Kedziora-Chudczer, et al. 2001, *The ATCA intraday variability survey of extragalactic radio sources*, *MNRAS* **325**, 1411

[8] K. I. Kellermann & I. I. K. Pauliny-Toth 1969, *The Spectra of Opaque Radio Sources*, *ApJ* **155**, 71

[9] J. G. Kirk & O. Tsang 2006, *High brightness temperatures and circular polarisation in extra-galactic radio sources*, *A&A* **447**, 13

[10] Y. Y. Kovalev, et al. 2002, *Broad-band Radio Spectra Variability of 550 AGN in 1997-2001*, *PASA* **19**, 83

[11] A. Kraus, et al. 2003, *Intraday variability in compact extragalactic radio sources. II. Observations with the Effelsberg 100 m radio telescope*, *A&A* **401**, 161

[12] M. L. Lister & D. C. Homan 2005, *MOJAVE: Monitoring of Jets in Active Galactic Nuclei with VLBA Experiments. I. First-Epoch 15 GHz Linear Polarization Images*, *AJ* **130**, 1389

[13] J. E. J. Lovell, et al. 2003, *First Results from MASIV: The Microarcsecond Scintillation-induced Variability Survey*, *AJ* **126**, 1699

[14] J.-P. Macquart & D. L. Jauncey 2002, *Microarcsecond Radio Imaging using Earth-Orbit Synthesis*, *ApJ* **572**, 786

[15] B. J. Rickett 1990, *Radio propagation through the turbulent interstellar plasma*, *ARA&A* **28**, 561

[16] A. Quirrenbach, et al. 1991, *Correlated radio and optical variability in the BL Lacertae object 0716+714*, *ApJ* **372**, 71

[17] T. Savolainen & Y. Y. Kovalev 2008, *Serendipitous VLBI detection of rapid large-amplitude intraday variability in QSO 1156+295*, *A&A*, submitted

[18] P. Sreekumar, et al. 1996, *EGRET Observations of the North Galactic Pole Region*, *ApJ* **464**, 628

[19] S. J. Wagner & A. Witzel 1995, *Intraday Variability In Quasars and BL Lac Objects*, *ARA&A* **33**, 163

[20] B. J. Wills, et al. 1983, *The QSO 1156+295 - A multifrequency study of recent activity*, *ApJ* **274**, 62